JOURNAL OF GUIDANCE, CONTROL, AND DYNAMICS
Vol. 16, No. 4, July–August 1993

Goddard Problem in Presence of a Dynamic Pressure Limit

Hans Seywald*
Analytical Mechanics Associates, Inc., Hampton, Virginia 23666
and
Eugene M. Cliff†
Virginia Polytechnic Institute and State University, Blacksburg, Virginia 24061

The Goddard problem is that of maximizing the final altitude for a vertically ascending, rocket-powered vehicle under the influence of an inverse square gravitational field and atmospheric drag. The present paper deals with the effects of two additional constraints, namely, a dynamic pressure limit and specified final time. Nine different switching structures involving zero-thrust arcs, full-thrust arcs, singular-thrust arcs, and state-constrained arcs are obtained when the value of the dynamic pressure limit is varied between zero and infinity and the final time is specified between the minimum possible time within which all of the fuel can be burned and the natural final time that emerges for the problem with final time unspecified. For all points in the aforementioned domain of dynamic pressure limit and prescribed final time, the associated optimal switching structure is clearly identified. Finally, a simple intuitive feedback law is presented for the free time problem. For all values of prescribed dynamic pressure limit, this strategy yields a loss in final altitude of less than 3% with respect to the associated optimal solution.

I. Introduction

THE problem of maximizing the final altitude for a vertically ascending rocket was first formulated by Goddard[1] in 1919. Numerous authors such as Hamel[2] in 1927, Tsien and Evans[3] in 1951, Miele and Cavoti[4] in 1958, Leitmann[5-9] in 1956–63, and Garfinkel[10] in 1963 have analyzed the problem using various mathematical methods and assumptions on the equations of motion. An extensive study of the problem under realistic assumptions on the equations of motion has become possible only with the development of the theory of optimal control in conjunction with powerful digital computers. Recently, Tsiotras and Kelley[11,12] have studied the effects of a final time specification and drag modeling.

In the present treatment, a dynamic pressure constraint, which in the context of optimal control represents a first-order state inequality constraint, is introduced to the problem. The effect of this constraint as well as the effect of restrictions on the final time are investigated for their impact on the switching structure and the maximum attainable altitude.

II. Problem Formulation

The problem is to maximize the final altitude for a rocket ascending vertically under the influence of atmospheric drag and an inverse square gravitational field. The states are radial distance r, velocity v, and mass m. The thrust magnitude T is the only control and is subject to fixed bounds $0 \le T \le T_{\max}$ (control constraints) and a dynamic pressure limit $q \le q_{\max}$ (state constraint). The following assumptions are made: point-mass model, Newtonian central gravitational field, one-dimensional trajectory, air density that varies exponentially with altitude, constant drag coefficient, and constant exhaust velocity.

In nondimensional form, the problem is given as follows:

$$\min -r(t_f) \tag{1}$$

subject to the equations of motion

$$\dot{r} = v$$

$$\dot{v} = \frac{T-D}{m} - \frac{1}{r^2}$$

$$\dot{m} = -\frac{T}{c} \tag{2}$$

the control constraint

$$T \in [0, T_{\max}] \tag{3}$$

the boundary conditions

$$r(0) = 1 \tag{4a}$$

$$v(0) = 0 \tag{4b}$$

$$m(0) = 1 \tag{4c}$$

$$r(t_f) \text{ to be maximized} \tag{4d}$$

$$v(t_f) \text{ free} \tag{4e}$$

$$m(t_f) = m_f \tag{4f}$$

and the state inequality constraint

$$P_0(r, v) = v - v_{\max}(r) \le 0 \tag{5}$$

where $v_{\max}$ is a prescribed smooth function of radial distance r.

III. Dynamic Pressure Limit

In Eq. (5), a state constraint of the general form $v \le v_{\max}(r)$ is introduced. With the functional dependence of $v_{\max}$ on the radial distance r given by

$$v_{\max}(r) := \sqrt{\frac{2q_{\max}}{\rho_0 e^{\beta(1-r)}}} \tag{6}$$

this represents a dynamic pressure limit $q \le q_{\max}$. It is interesting to note that many other state constraints of practical inter-

Received Dec. 2, 1991; revision received July 21, 1992; accepted for publication Sept. 1, 1992.

*Senior Project Engineer, 17 Research Drive; working under contract at the Spacecraft Controls Branch, NASA Langley Research Center. Member AIAA.

†Reynolds Metals Professor, Interdisciplinary Center for Applied Mathematics. Associate Fellow AIAA.

est, such as a Mach limit or a heating rate constraint, can be represented in the same general form of Eq. (5). All state constraints of the form of Eq. (5) are of order 1 and, except for the explicit functional dependence of $v_{\max}$ on r, involve the same optimality conditions and require the same techniques for numerical treatment.

IV. Drag Model and Vehicle Data

The variables in the system description of Eqs. (1–6) are nondimensionalized with $\bar{r}$ = Earth's radius as the length scale, $\bar{m}$ = initial mass of the vehicle as the mass scale, and $\bar{t} = \sqrt{\bar{r}/g}$ as the time scale. Here $g = 9.80665$ m/s^2 denotes the value of Earth's gravitational acceleration at radius $\bar{r}$. The explicit numerical values of $\bar{r}$ and $\bar{t}$ are

$$\bar{r} = 6.37 \cdot 10^6 \text{ m}$$

$$\bar{t} = 805.95 \text{ s}$$

These are the usual canonical units used in astrodynamics.[13] Note that the unit speed corresponds to circular orbit speed at the Earth's surface ($\sim$7.9 km/s).

The symbols T and D in Eq. (2) denote the ratios of thrust to initial weight and drag to initial weight, respectively. This nondimensional drag is given by

$$D = \frac{qC_DA}{m_0 g}$$

where

$$q = \tfrac{1}{2}\rho v^2$$

and

$$\rho = \rho_0 e^{\beta(1-r)}$$

denote the dynamic pressure and air density, respectively. The constants C_D, A, and m_0 denote drag coefficient, reference area, and initial mass, respectively. Additionally, ρ_0, β, c, and m_f are air density at sea level, density decay rate, exhaust velocity, and final mass, respectively. The drag model involves the parameter $\rho_0 C_D A/m_0 g$. The values used for numerical calculations are

$$T_{\max} = 3.5$$

$$m_f = 0.6$$

$$\beta = 500$$

$$c = 0.5$$

$$\frac{\rho_0 C_D A}{m_0 g} = 620 \tag{7}$$

These values are adopted from Ref. 14 and roughly correspond to a Soviet SA-2 surface-to-air missile, NATO code named GUIDELINE. The dimensional value of the dynamic pressure is obtained from

$$q^{\text{dimensional}} = (q \cdot A) \cdot 6174 \text{ N}$$

The explicit value of the cross section area A is not given in Ref. 14.

V. Minimum Principle

Problem (1–6) is solved by applying the Pontryagin minimum principle. Assuming that a solution of Eqs. (1–6) exists, the minimum principle states that at every point in time the control is such that the variational Hamiltonian

$$H(r, v, m, \lambda_r, \lambda_v, \lambda_m) = \lambda_r \dot{r} + \lambda_v \dot{v} + \lambda_m \dot{m} \tag{8}$$

is minimized subject to all control constraints:

$$T = \arg\min_{T \in U} H, \qquad U = \{T \in R \mid T \text{ admissible}\} \tag{9}$$

On unconstrained arcs (i.e., on time intervals where Eq. (5) is satisfied with strict inequality),

$$U = \{T \in R \mid 0 \le T \le T_{\max}\} \tag{10}$$

On constrained arcs (i.e., on time intervals, say $[\tau_1, \tau_2]$, where Eq. (5) is satisfied with strict equality),

$$P_0 \equiv 0 \quad \text{on} \quad [\tau_1, \tau_2] \tag{11}$$

is equivalent to

$$P_0 = 0 \quad \text{at} \quad t = \tau_1 \tag{12}$$

$$P_1 \equiv 0 \quad \text{on} \quad t \in (\tau_1, \tau_2) \tag{13}$$

where

$$P_1 := \frac{dP_0}{dt} = \frac{T-D}{m} - \frac{1}{r^2} - v'_{\max}(r)v \tag{14}$$

(here and in the remainder of this paper the prime denotes differentiation with respect to radial distance r) so that the set of admissible controls is

$$U = \{T \in R \mid 0 \le T \le T_{\max}, \quad P_1 = 0\} \tag{15}$$

For a fixed state vector, this set usually consists of a single point but may be empty. The evolution of the Lagrange multipliers λ_x, $x \in \{r, v, m\}$, is governed by

$$\dot{\lambda}_x = -\frac{\partial H}{\partial x} \tag{16}$$

on unconstrained arcs. On constrained arcs, the implicit dependence of the control on states via Eq. (13) implies

$$\dot{\lambda}_x = -\frac{\partial H}{\partial x} - \mu \frac{\partial P_1}{\partial x} \tag{17}$$

(see Bryson et al.[15]) where μ is the Kuhn-Tucker multiplier in the minimization (9) subject to Eq. (10). Supplementary optimality conditions are given by

$$\mu \ge 0 \tag{18}$$

$$\dot{\mu} \le 0 \tag{19}$$

(see Jacobson et al.[16]).

VI. Hamiltonian and Adjoint Equations

Explicitly the Hamiltonian (8) takes the form

$$H = \lambda_r v + \lambda_v\left(\frac{T-D}{m} - \frac{1}{r^2}\right) - \lambda_m \frac{T}{c} \tag{20}$$

and the adjoint equations are

$$\dot{\lambda}_r = \frac{\lambda_v}{m}\frac{\partial D}{\partial r} - \lambda_v \frac{2}{r^3} - \mu\left[-\frac{1}{m}\frac{\partial D}{\partial r} + \frac{2}{r^3} - v''_{\max}(r)v\right]$$

$$\dot{\lambda}_v = \frac{\lambda_v}{m}\frac{\partial D}{\partial v} - \lambda_r - \mu\left[-\frac{1}{m}\frac{\partial D}{\partial v} - v'_{\max}(r)\right]$$

$$\dot{\lambda}_m = \frac{\lambda_v}{m^2}(T-D) - \mu\left(-\frac{T-D}{m^2}\right) \tag{21}$$

where on unconstrained arcs

$$\mu = 0 \tag{22}$$

and on constrained arcs

$$\frac{\partial H}{\partial T} + \mu \frac{\partial P_1}{\partial T} = 0 \tag{23}$$

VII. Control Logic

With the switching function S defined by

$$S := \frac{\partial H}{\partial T} = \frac{\lambda_v}{m} - \frac{\lambda_m}{c} \tag{24}$$

the minimum principle (9) and (10) implies

$$T = \begin{cases} 0 & \text{if } S > 0 \\ T_{\max} & \text{if } S < 0 \\ T_{\text{sing}} & \text{if } S \equiv 0 \end{cases} \tag{25}$$

On singular arcs $S = 0$, $\dot{S} = 0$, and $\ddot{S} = 0$ imply

$$\lambda_v - \lambda_m \frac{m}{c} = 0 \tag{26}$$

$$\lambda_r - \frac{\lambda_m}{c}\left(\frac{\partial D}{\partial v} + \frac{D}{c}\right) = 0 \tag{27}$$

and

$$T_{\text{sing}} = \frac{A_1 + A_2}{A_3} \tag{28}$$

where

$$A_1 = -\frac{D}{mc}\left(\frac{\partial D}{\partial v} + \frac{D}{c}\right) + \frac{\partial^2 D}{\partial v \partial r} v - \frac{\partial^2 D}{\partial v^2}\left(\frac{D}{m} + \frac{1}{r^2}\right)$$

$$A_2 = \frac{1}{c}\left[\frac{\partial D}{\partial r} v - \frac{\partial D}{\partial v}\left(\frac{D}{m} + \frac{1}{r^2}\right)\right] + \left(\frac{\partial D}{\partial r} + \frac{2m}{r^3}\right)$$

and

$$A_3 = \frac{1}{mc}\left(\frac{\partial D}{\partial v} + \frac{D}{c}\right) + \frac{\partial^2 D}{\partial v^2}\frac{1}{m} + \frac{\partial D}{\partial v}\frac{1}{mc}$$

respectively. The singular arc is of first order (see Bryson and Ho[17]). On state-constrained arcs of Eq. (9), Eq. (15) implies

$$\mu = -\lambda_v + \lambda_m \frac{m}{c} \qquad \left(\text{from } \frac{\partial H}{\partial T} + \mu \frac{\partial P_1}{\partial T} = 0\right) \tag{29}$$

$$T_{\text{constr}} = D + \frac{m}{r^2} + m v'_{\max}(r) v \qquad (\text{from } P_1 = 0) \tag{30}$$

Along singular arcs the generalized Legendre-Clesch condition (see Kelley et al.[18]),

$$(-1)^q \frac{\partial}{\partial T}\left[\frac{\mathrm{d}^{2q}}{\mathrm{d}t^{2q}}\left(\frac{\partial H}{\partial T}\right)\right] \geq 0, \qquad q = 1 \tag{31}$$

yields

$$-\frac{\lambda_m}{mc}\left[\frac{1}{mc}\left(\frac{\partial D}{\partial v} + \frac{D}{c}\right) + \frac{\partial^2 D}{\partial v^2}\frac{1}{m} + \frac{\partial D}{\partial v}\frac{1}{mc}\right] \geq 0 \tag{32}$$

and is checked numerically.

VIII. Transversality and Corner Conditions

All transversality and corner conditions are given such that the first variation δJ of the cost function of Eq. (1), $J = -r(t_f)$, is zero.[16,17] For the boundary conditions of Eq. (4), this yields

$$\lambda_r(t_f) = -1 \tag{33}$$

$$\lambda_v(t_f) = 0 \tag{34}$$

In case of free final time t_f, the associated optimality condition is

$$H(t_f) = 0 \tag{35}$$

As no explicitly time-dependent interior point constraints are imposed on the problem, the Hamiltonian H is continuous throughout the time interval $[0, t_f]$, including across corners. At switching points between minimum and maximum thrust T this implies

$$S = 0 \tag{36}$$

where S is the switching function given in Eq. (24).

At the beginning of singular arcs, conditions in Eqs. (26) and (27) must be satisfied to guarantee that control logic of Eq. (28) keeps the switching function of Eq. (24) identically zero. Note that singular arcs may occur naturally as part of an optimal solution but their existence cannot be forced. Consequently, even though conditions of Eqs. (26) and (27) can be used for the numerical calculation of a trajectory involving singular control arcs, these conditions cannot be considered as physically imposed constraints on the problem and hence do not lead to any jumps in the costates or the Hamiltonian.

At the beginning, say t_1, of the state-constrained arc, conditions are

$$P_0(t_1) = 0 \tag{37a}$$

$$S(t_1^-)\left[T(t_1^+) - T(t_1^-)\right] = 0 \tag{37b}$$

$$\lambda_r(t_1^+) = \lambda_r(t_1^-) - l_0 \frac{\partial P_0}{\partial r} \tag{37c}$$

$$\lambda_v(t_1^+) = \lambda_v(t_1^-) - l_0 \frac{\partial P_0}{\partial v} \tag{37d}$$

$$\lambda_m(t_1^+) = \lambda_m(t_1^-) - l_0 \frac{\partial P_0}{\partial m} \tag{37e}$$

where superscripts + and − denote evaluation at times $t_1 + \epsilon$, $t_1 - \epsilon$, $\epsilon > 0$, and $\epsilon \to 0$, respectively. The end, say t_2, of the constrained arc is determined by

$$S(t_2^-)\left[T(t_2^+) - T(t_2^-)\right] = 0 \qquad \text{at} \quad t = t_2 \tag{38}$$

Conditions (37b) and (38) are equivalent to the continuity of the Hamiltonian at t_1 and t_2, respectively. This can be easily verified by writing the Hamiltonian (20) in the form $H(x, \lambda, u) = H_0(x, \lambda) + S(x, \lambda) \cdot T$ and noting that all states and costates and consequently also H_0 and S are continuous across t_1 and t_2. Note that two solutions, namely, $S^- = 0$ and $T^+ - T^- = 0$, are possible. The jump in the multipliers (37c), (37d), and (37e) is implied by the interior point condition, Eq. (37a).

IX. Numerical Results

For a numerical treatment of the problem, the dynamic pressure limit $q_{\max}$ (or equivalently $q_{\max} \cdot A$) is varied between $q_{\max} = 0$ (trivial case in which a rocket is allowed only hovering with maximum velocity zero) and $q_{\max} = +\infty$ (dynamic pressure limit can be ignored). In the fixed final time case, t_f is prescribed explicitly with values between $t_{f,\min}$, the minimum

time within which all fuel can be burned, and t_f^*, the optimal free final time. There is no point in considering specified times larger than t_f^*, since one imagines the vehicle could simply be held on the launch pad until t_f^* time units remain. In the free final time case always $v(t_f^*)=0$ is obtained, i.e., the final velocity is zero.

As noted earlier, the switching structure, that is, the sequence of different control logics that actually solves the problem, is not known in advance. For a given problem it has to be found by numerical experiments. Assuming a certain switching structure, the state equations (2), costate equations (21), along with boundary conditions (4a–4c) and (4f), transversality conditions (33) and (34), and corner conditions implied by the assumed switching structure yield a multipoint boundary-value problem (see Fig. 1 for an example case). For $q_{\max}>0$ and t_f ranging between the minimum possible flight time $t_{f,\min}(q_{\max})$ within which all of the fuel can be burned and the optimal flight time $t_f^*(q_{\max})$, the following different switching structures are found to solve the problem:

S1) full-zero
S2) full-singular-zero
S3) full-singular-full-zero
S4) full-constrained-zero
S5) full-constrained-singular-zero
S6) full-constrained-singular-full-zero
S7) full-constrained-full-zero
S8) full-constrained-full-singular-zero
S9) full-constrained-full-singular-full-zero

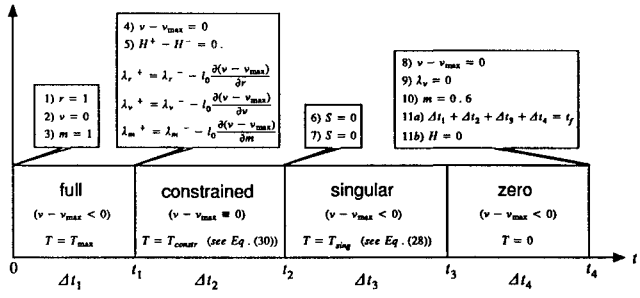

Fig. 1 Schematic representation of the boundary-value problem associated with the switching structure: full, constrained, singular, and zero.

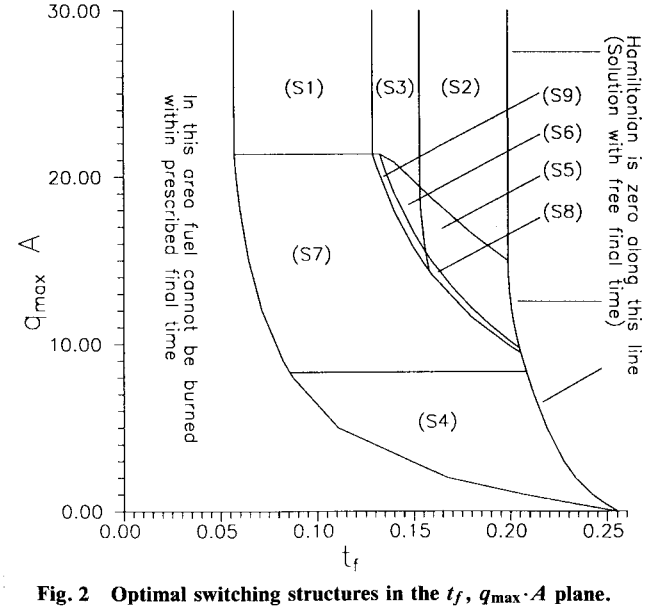

Fig. 2 Optimal switching structures in the t_f, $q_{\max}\cdot A$ plane.

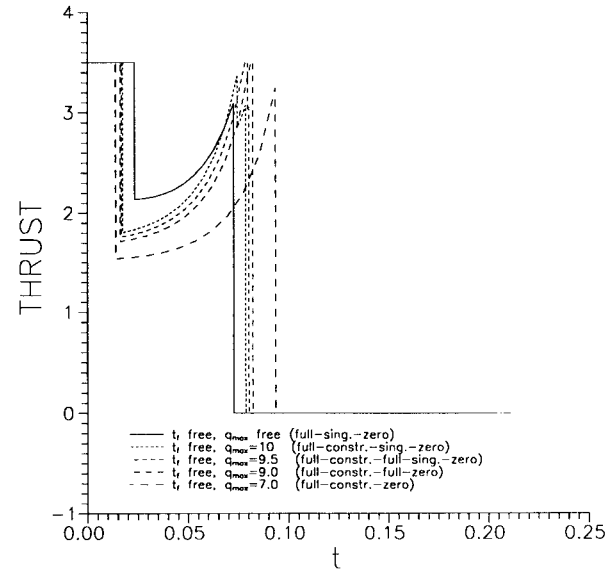

Fig. 3 Thrust vs time for selected trajectories in the free time case.

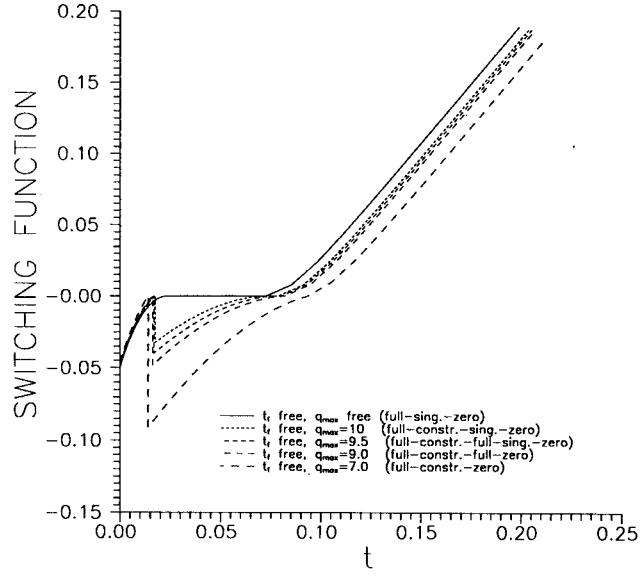

Fig. 4 Switching function vs time for selected trajectories in the free time case.

For switching structures S4, S5, and S6, the continuity of the Hamiltonian at the end of the constrained arc, say at time t_2, imposed by condition (38) is satisfied through $S^-=0$ (or equivalently $\mu^-=0$). For switching structures S7, S8, and S9, condition (38) is satisfied through $T^+-T^-=0$. The domains in the $t_f, q_{\max}$ plane where the previous switching structures solve Eqs. (1–6) are shown in Fig. 2. The time histories of thrust T, the switching function S, and the dynamic pressure times cross section area $q\cdot A$, for selected trajectories in the free time case, are given in Figs. 3–5, respectively. Figure 6 shows the same trajectories in the h,v plane in dimensional units.

X. Numerical Procedure for Solving Multipoint Boundary-Value Problems

For switching structure S5 (full-constrained-singular-zero) the multipoint boundary-value problem (MPBVP) associated with the first-order necessary conditions is indicated schematically in Fig. 1. This is the simplest switching structure that involves each one of the possible control logics at least once.

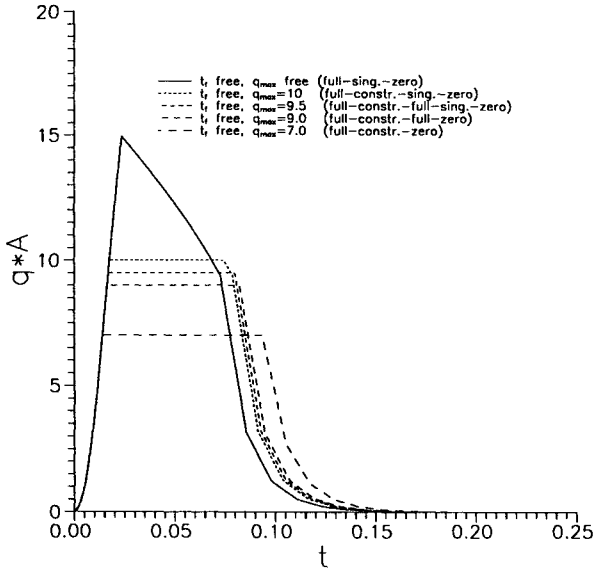

Fig. 5 Dynamic force $q \cdot A$ vs time for selected trajectories in the free time case.

It is clear that the trajectory can be obtained by simple forward integration once all parameters $r(0)$, $v(0)$, $m(0)$, $\lambda_r(0)$, $\lambda_v(0)$, $\lambda_m(0)$, l_0, Δt_1, Δt_2, Δt_3, and Δt_4 are known. These 11 parameters are determined by the 11 conditions numbered 1–10 and 11a for fixed final time and 1–10 and 11b for free final time in Fig. 1, respectively. (The jump conditions for the Lagrange multipliers at time t_1 can be considered directly during the integration.) The smoothness of the right-hand side of the differential equations on each subarc implies smooth dependence of all conditions on the parameters, so that a Newton method can be applied to solve this root-finding problem.

Despite its simple structure, the Goddard problem is not an easy problem to solve. A first optimal trajectory for problems (1) and (4) can be generated by explicitly prescribing final time t_f and assuming switching structure S1 (full-zero). From Fig. 2 it is clear that this is the correct switching structure provided the final time t_f is prescribed sufficiently small and $q_{\max}A$ is sufficiently large. The associated MPBVP is well conditioned, and the Newton method converges well, even with trivial initial guesses, such as $\lambda_r(0)=1$, $\lambda_v(0)=1$, $\lambda_m(0)=1$, $\Delta t_1=0$, $\Delta t_2=0$, $\Delta t_3=0$, and $\Delta t_4=0$. (The notation used here is analogous to the one used in Fig. 1.) Subsequently, using continuation methods, the prescribed final time can be increased until the optimal final time t_f^* is reached. By monitoring the behavior of the switching function S and its first time derivative $\dot{S}$, it is always possible to guess the correct switching structure.

The dynamic pressure limit (5) and (6) can be introduced to the problem by starting at a solution with switching structure S1 (full-zero) and prescribing the maximum dynamic pressure $q_{\max}$ slightly below the maximum q value obtained in the solution to the free problem. By monitoring the switching function, its derivative, and the dynamic pressure function of time along the solutions obtained, it is always possible to guess the correct switching structure when changing $q_{\max}$ and t_f in a continuation method with sufficiently small steps.

In most cases the convergence of the associated MPBVPs is good once the switching structure is guessed correctly. In some cases the convergence is bad. For all but two switching structures, namely, S3 (full-singular-full-zero) and S9 (full-constrained-full-singular-full-zero), the bad convergence can be overcome by simply reducing the step size in the continuation method. For switching structures S3 and S9, this cannot solve the problem when the length of the full-thrust arc following the singular-thrust arc is sufficiently small. The sources for the numerical difficulties are the same for both switching structures and lie in the fact that the switching function is very flat and small in magnitude along the full-thrust arc following the singular arc. If this full-thrust arc is short, this causes the switching time that determines the end of the full-thrust arc to be extremely badly conditioned. Even multiple shooting (see Stoer and Bulirsch[19]) cannot alleviate this problem satisfactorily.

A remedy for this problem is to start the integration at the end of the singular-thrust arc. Explicitly, consider switching structure S3 (full-singular-full-zero) and let 0, t_1, t_2, t_3, and $t_4=t_f$ denote the initial time, the three interior switching times, and the final time, respectively. At the end of the singular control arc, i.e., at time t_2, it is known that conditions (26) and (27) must hold. Starting the integration at time t_2, these conditions can be used to express Lagrange multipliers $\lambda_r(t_2)$ and $\lambda_v(t_2)$ in terms of the remaining states and costates. Hence the set of parameters

$$r(t_2) \quad v(t_2) \quad m(t_2) \quad \lambda_m(t_2)$$
$$\Delta t_1 \quad \Delta t_2 \quad \Delta t_3 \quad \Delta t_4 \tag{39}$$

completely characterizes the trajectory. These eight parameters are determined through the following eight conditions:

$$r(0) = 1 \tag{40a}$$
$$v(0) = 0 \tag{40b}$$
$$m(0) = 1 \tag{40c}$$
$$S(t_3) = 0 \tag{40d}$$
$$\lambda_r(t_f) = -1 \tag{40e}$$
$$\lambda_v(t_f) = 0 \tag{40f}$$
$$m(t_f) = 0.6 \tag{40g}$$
$$\Delta t_1 + \Delta t_2 + \Delta t_3 + \Delta t_4 = t_f \tag{40h}$$
$$H(t_f) = 0 \tag{40i}$$

Here the conditions (40h) and (40i) refer to fixed and free final time cases, respectively. The boundary-value problem of Eqs. (39) and (40) is well conditioned, and convergence can be obtained even if $t_3 - t_2 < 10^{-4}$. In this case, $|S| < 10^{-10}$ on the integral (t_2, t_3).

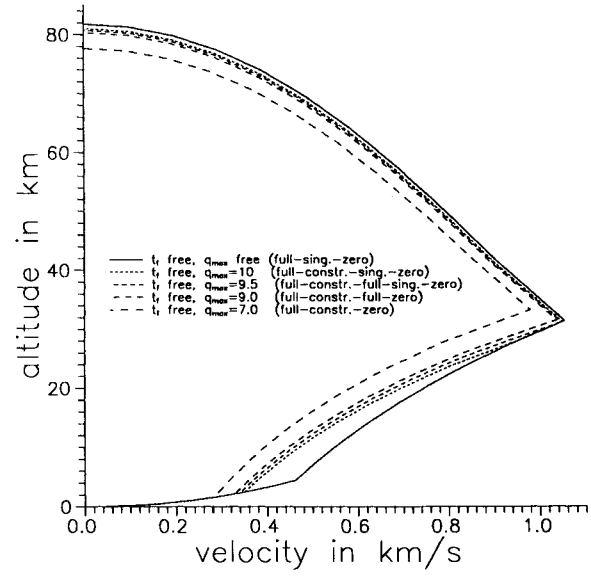

Fig. 6 Altitude-velocity chart for selected trajectories in the free time case.

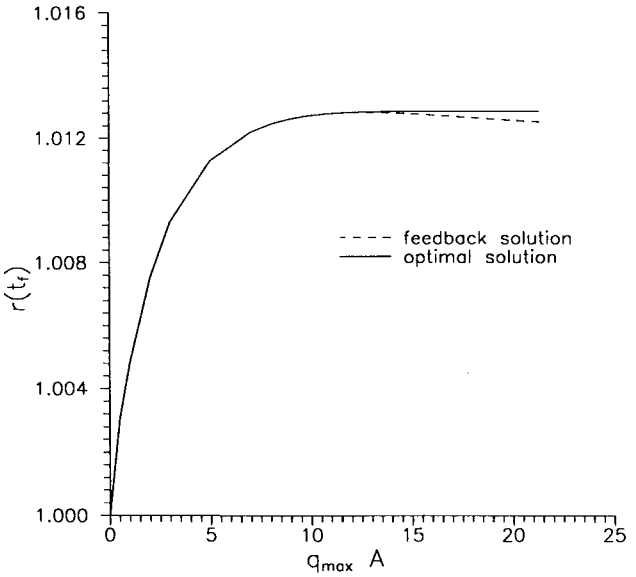

Fig. 7 Payoff vs dynamic pressure limit comparing the optimal solution and the feedback solution.

XI. Simple Feedback Strategy

An intuitive feedback law to solve the problem of Eqs. (1–6) with free final time t_f is given as follows: choose T as large as possible subject to the constraints $T \in [0, T_{\max}]$ and $P_0 = q - q_{\max} \leq 0$. That means the thrust is always set $T = T_{\max}$ and is reduced to the value computed by expression (30) whenever the dynamic pressure limit $P_0 = 0$ is active. The optimal final time t_f^* is obtained from $v(t_f^*) = 0$. The structure of these feedback solutions is found to be of the following form:

(FB0) constr.	if	$q_{\max} \cdot A = 0$
(FB1) full-constr.-zero	if	$q_{\max} \cdot A \in (0, 8.303)$
(FB2) full-constr.-full-zero	if	$q_{\max} \cdot A \in (8.303, 21.334)$
(FB2) full-zero	if	$q_{\max} \cdot A > 21.334$

By comparison with the optimal switching structures given in Fig. 2, it is found that these feedback strategies actually yield the optimal solution for $q_{\max} \cdot A < 8.303$. For $q_{\max} \cdot A > 8.303$, the loss in final altitude increases until $q_{\max,\text{free}} \cdot A = 21.334$, the maximum attainable dynamic force with thrusters burning on full throttle, is reached. For $q_{\max} > q_{\max,\text{free}}$, the loss in performance remains constant. These results are shown in Fig. 7. It is observed that the relative loss in final altitude never exceeds 2.5%.

XII. Conclusion

The effect of a dynamic pressure constraint on the vertical ascent of a sounding rocket has been studied. Trajectories leading to maximum possible altitudes have been obtained for arbitrarily prescribed values of the dynamic pressure limit and for specified final times ranging between the minimum possible time within which all of the fuel can be burned and the optimal final time that emerges for the problem if the final time is left free. Nine different switching structures have been obtained and the domain of dynamic pressure limit and specified final time where they furnish the optimal solutions have been clearly identified. It has been shown how, at times, the condition of MPBVPs associated with the first-order necessary conditions can be improved dramatically by starting the integration at a conveniently chosen point in the interior of the trajectory. Finally the optimal solutions in the free-time case have been compared with a simple intuitive feedback strategy.

Acknowledgments

This work was supported in part by NASA Langley Research Center under Grant NAG-1-946, D. Moerder, technical monitor, and in part by the Defense Advance Research Projects Agency under the Applied and Computational Mathematics Program Contract F49620-87-C-0016.

References

[1]Goddard, R. H., "A Method of Reaching Extreme Altitudes," Smithsonian Int. Misc. Collections 71,1919; also American Rocket Society, 1946.

[2]Hamel, G., "Über eine mit dem Problem der Rakete zusammenhängende Aufgabe der Variationsrechnung," *Zeitschrift für Angewandte Mathematik and Mechanik,* Vol. 7, No. 6, 1927, pp. 451, 452 (in German).

[3]Tsien, H. S., and Evans, R. C., "Optimum Thrust Programming for a Sounding Rocket," *Journal of American Rocket Society,* Vol. 21, No. 5, 1951, pp. 99–107.

[4]Miele, A., and Cavoti, C. R., "Generalized Variational Approach to the Optimum Thrust Programming for the Vertical Flight of a Rocket," *Zeitschrift für Flugwissenschaften,* Vol. 6, No. 4, 1958, pp. 102–109.

[5]Leitmann, G., "A Calculus of Variations Solution of Goddard's Problem," *Astronautica Acta,* Vol. 2, No. 2, 1956, pp. 55–62.

[6]Leitmann, G., "Optimum Thrust Programming for High Altitude Rockets," *Aeronautical Engineering Review,* Vol. 16, No. 6, 1957, pp. 63–66.

[7]Leitmann, G., "Stationary Trajectories for a High-Altitude Rocket with Drop-Away Booster," *Astronautica Acta,* fasc. 3, 1956, pp. 119–124.

[8]Leitmann, G., "On a Class of Variational Problems in Rocket Flight," *Journal of Aero/Space Science,* Vol. 26, No. 9, Sept. 1959, pp. 586–591.

[9]Leitmann, G., "An Elementary Derivation of the Optimal Control Conditions," *12th International Astronautical Congress,* Academic Press, New York, 1963.

[10]Garfinkel, B., "A Solution of the Goddard Problem," *SIAM Journal on Control,* Vol. 1, No. 3, 1963, pp. 349–368.

[11]Tsiotras, P., and Kelley, H. J., "Goddard Problem with Constrained Time of Flight," *Journal of Guidance, Control, and Dynamics,* Vol. 15, No. 2, 1992, pp. 289–296.

[12]Tsiotras, P., and Kelley, H. J., "Drag Law Effects in the Goddard Problem," IFAC Optimzation Workshop, Tblisi, Georgia, USSR, June 21–25, 1988.

[13]Bate, R. R., Mueller, D. D., and White, J. E., *Fundamentals of Astrodynamics,* Dover, New York, 1971.

[14]Zlatskiy, V. T., and Kiforenko, B. N., "Optimum Trajectories with Singular Arcs," *Automation and Remote Control,* Vol. 35, No. 12, Pt. 1, Dec. 1974, pp. 1885–1890.

[15]Bryson, A. E., Denham, W. F., and Dreyfus, S. E., "Optimal Programming Problems with Inequality Constraints, I—Necessary Conditions for Extremal Solutions," *AIAA Journal,* Vol. 1, No. 11, 1963, pp. 2544–2550.

[16]Jacobson, D. H., Lele, M. M., and Speyer, J. L., "New Necessary Conditions of Optimality for Control Problems with State-Variable Inequality Constraints," *Journal of Mathematical Analysis and Applications,* Vol. 35, No. 2, Aug. 1971, pp. 255–284.

[17]Bryson, A. E., and Ho, Y. C., *Applied Optimal Control,* Hemisphere, New York, 1975.

[18]Kelley, H. J., Kopp, R. E., and Moyer, H. G., "Singular Extremals in Optimal Control," *Optimization Techniques,* Vol. 2, edited by G. Leitmann, Academic Press, New York, 1967.

[19]Stoer, J., and Bulirsch, R., *Introduction to Numerical Analysis,* Springer-Verlag, New York, 1980.